

Structural relaxation and delayed yielding in cyclically sheared Cu-Zr metallic glasses

Nikolai V. Priezjev^{1,2}

¹*Department of Civil and Environmental Engineering,
Howard University, Washington, D.C. 20059 and*

²*Department of Mechanical and Materials Engineering,
Wright State University, Dayton, OH 45435*

(Dated: July 24, 2024)

Abstract

The yielding transition, structural relaxation, and mechanical properties of metallic glasses subjected to repeated loading are examined using molecular dynamics simulations. We consider a poorly-annealed Cu-Zr amorphous alloy periodically deformed in a wide range of strain amplitudes at room temperature. It is found that low-amplitude cyclic loading leads to a logarithmic decay of the potential energy, and lower energy states are attained when the strain amplitude approaches a critical point from below. Moreover, the potential energy after several thousand loading cycles is a linear function of the peak value of the stress overshoot during startup continuous shear deformation of the annealed sample. We show that the process of structural relaxation involves collective, irreversible rearrangements of groups of atoms whose spatial extent is most pronounced at the initial stage of loading and higher strain amplitudes. At the critical amplitude, the glass becomes mechanically annealed for a number of transient cycles and then yields via formation of a shear band. The yielding transition is clearly marked by abrupt changes in the potential energy, storage modulus, and fraction of atoms with large nonaffine displacements.

Keywords: yielding transition, metallic glasses, plastic deformation, cyclic loading, molecular dynamics simulations

I. INTRODUCTION

Establishing structure-property-performance relations for bulk metallic glasses is important for various structural and functional applications [1, 2]. Owing to their amorphous atomic structure, metallic glasses offer a number of unique properties, such as high strength, large elastic limit, as well as superior wear and corrosion resistance [3, 4]. An outstanding challenge that limits their widespread use is that sufficiently well annealed glasses are prone to brittle failure via formation of nanoscale shear bands [5]. In addition, metallic glasses subjected cyclic variations in stresses or strains exhibit relatively low fatigue limit and fatigue life, which can be affected by the sample size, chemical composition, cycling frequency, and surface conditions [6–8]. To enhance their ductility, metallic glasses can be rejuvenated using several thermo-mechanical processing methods, including high-pressure torsion, ion irradiation, thermal cycling, cold rolling, and elastostatic loading [9, 10]. Alternatively, an atomic structure can be simply reset by heating above the glass transition temperature and subsequent rapid cooling to the glass state or a supercooled glass former can be frozen under applied stress [11, 12]. In recent years, laser-based additive manufacturing techniques were also introduced to fabricate large-scale complex structures and patient-specific implants for biomedical applications [13]. Despite these advances, however, development of novel processing methods to rejuvenate metallic glasses and improve their mechanical properties remains a challenging task.

In the last decade, a number of molecular dynamics (MD) simulation studies have investigated the yielding behavior and structural relaxation in amorphous solids subjected to oscillatory deformation [14–46]. Notably, it was demonstrated that in the athermal limit, binary Lennard-Jones (LJ) glasses under low-amplitude loading gradually evolve into periodic limit cycles with exactly reversible trajectories of atoms [15, 17], and the potential energy of such states is lower for better annealed glasses and higher strain amplitudes [16, 23]. By contrast, periodic shear deformation in combination with thermal noise facilitate collective, irreversible rearrangements of atoms and prolonged structural relaxation [39, 40]. In addition, lower energy states can be accessed when cyclic shear is periodically alternated along two or three mutually perpendicular planes [30, 43]. Moreover, the range of energy states attainable in thermal glasses during low-amplitude loading can be extended by increasing strain amplitude slightly above a critical point every few cycles [36]. Furthermore,

when the loading amplitude exceeds a critical value, amorphous alloys undergo a yielding transition after a number of transient cycles [19, 23, 24, 27, 28, 31, 33, 34, 37, 40, 42, 44]. Interestingly, the critical strain amplitude in athermal systems might depend on the glass stability [32, 35], whereas at about half T_g , the yielding transition is delayed in better annealed glasses but the critical strain amplitude remains unchanged [40]. It was recently shown that well annealed binary glasses fail via shear band formation, and number of cycles to reach the yielding transition is well described by the power-law function of the difference between the strain amplitude and its critical value [42, 44]. However, the role of loading conditions and preparation history on the critical behavior of metallic glasses is not yet fully understood.

In this paper, the yielding behavior and structural relaxation in a Cu-Zr metallic glass under periodic shear deformation are studied using molecular dynamics simulations. We consider the binary glass that is first rapidly cooled across the glass transition to room temperature and then cyclically loaded in a wide range of strain amplitudes around a critical value. It will be shown that low-amplitude loading leads to a logarithmic decay of the potential energy during thousands of cycles. When the loading amplitude increases toward the critical value, the average size of plastically deformed domains becomes larger and the glass is relocated to lower energy states. On the contrary, we find that the yielding transition at the critical strain amplitude is marked by abrupt changes in the storage modulus, potential energy, and the number of atoms with large nonaffine displacements, which are localized within a narrow shear band.

The rest of this paper is structured as follows. The MD simulation setup, parameter values, as well as cooling and deformation protocols are described in the next section. The analysis of the potential energy, shear stress, and nonaffine displacements are presented in section III. A summary of the results is provided in the last section.

II. MD SIMULATIONS

In our study, the metallic glass was represented by a binary mixture of Cu and Zr atoms, which interacted via the embedded atom method (EAM) potentials [47, 48]. The total number of atoms in the $\text{Cu}_{50}\text{Zr}_{50}$ glass is 60 000. The preparation procedure consisted of several steps. First, the binary mixture was thoroughly equilibrated in a periodic box at

the temperature of 2000 K and zero pressure. This temperature is well above the glass transition temperature $T_g \approx 675$ K. We followed the cooling protocol by Fan and Ma [49], where the Cu-Zr system is initially cooled to 1500 K at the rate of 10^{13} K/s and then to 300 K at 10^{12} K/s. As a result, the effective cooling rate was 10^{12} K/s. The sample was prepared using the Nosé-Hoover thermostat, zero applied pressure, and periodic boundary conditions. The equations of motion were integrated with the time step $\Delta t = 1.0$ fs [50].

The periodic shear deformation was applied along the xz plane as follows:

$$\gamma_{xz}(t) = \gamma_0 \sin(2\pi t/T), \quad (1)$$

where γ_0 is the strain amplitude and T is the oscillation period. In our setup, the oscillation period was set to 1.0 ns (10^6 MD time steps), and the strain amplitude was varied in the range $0.020 \leq \gamma_0 \leq 0.061$. The MD simulations were carried out in the NVT ensemble with the temperature of 300 K and the linear size of the periodic box of 101.8 Å. A typical simulation of 4000 shear cycles took about 6000 hours using 40 processors in parallel. Due to computational limitations, the data for the potential energy, shear stress, and atomic configurations were collected for only one independent sample.

III. RESULTS

One of the key factors that strongly affects mechanical properties of metallic glasses is the rate of cooling during glass formation [9]. In general, glasses obtained by cooling at a slower rate become more stable and, upon deformation, exhibit a stress overshoot followed by plastic flow, whereas rapidly cooled glasses are settled at higher energy states and yield more smoothly [3]. Alternatively, it was recently demonstrated that poorly annealed LJ glasses can be relocated to lower energy states via low-amplitude cyclic loading at a finite temperature below T_g [39, 40]. However, the resulting change in the potential energy at given strain amplitude and temperature as well as the yielding behavior near the critical strain amplitude for more realistic models of glasses remain to be determined. In the present study, we considered the $\text{Cu}_{50}\text{Zr}_{50}$ glass that was first rapidly cooled to room temperature and then periodically strained for 4000 shear cycles over a broad range of strain amplitudes. This relatively large number of loading cycles was set based on the results of the previous MD study where a rapidly cooled binary LJ glass (60 000 atoms) yielded only after about

2500 cycles at a critical strain amplitude [33].

We first plot potential energy minima after each cycle at zero strain in Fig. 1 for strain amplitudes $0.020 \leq \gamma_0 \leq 0.055$. As is evident, the glass is relocated to progressively lower energy states upon continued loading, and cycle-to-cycle fluctuations are enhanced at larger strain amplitudes. Moreover, cyclic loading at higher strain amplitudes (up to a critical value) allows for rearrangement of larger clusters of atoms during each cycle, leading, on average, to more relaxed states. These conclusions are in agreement with the results of previous MD studies of binary LJ glasses [23, 26, 39, 40]. In Fig. 2, the same data for the potential energy as a function of the cycle number are replotted on a semi-log scale. It can be clearly observed that for each strain amplitude, the potential energy closely follows a logarithmic decay when $t/T \gtrsim 10$, suggesting a possibility of reaching lower energy states upon further loading. Interestingly, periodic deformation for 4000 shear cycles at $\gamma_0 = 0.055$ resulted in the potential energy $U \approx -4.951$ eV (see Fig. 2), which is nearly the same as in the case of a better annealed $\text{Cu}_{50}\text{Zr}_{50}$ glass prepared at a 100 times slower cooling rate [44]. In other words, the rapidly cooled glass (10^{12} K/s) was mechanically annealed to the potential energy level of a more slowly cooled glass (10^{10} K/s), which was considered in the previous MD study [44].

The variation of the potential energy during cyclic loading at higher strain amplitudes, $\gamma_0 \geq 0.055$, is presented in Fig. 3. For reference, the same data for $\gamma_0 = 0.055$ as in Fig. 1 are also included in Fig. 3 for the first 1300 cycles. It can be readily seen that, following a number of transient cycles, the potential energy abruptly increases, indicating shear band formation at the yielding transition. Note that except for a relatively large strain amplitude $\gamma_0 = 0.061$, rapidly cooled glass is mechanically annealed for a number of cycles before yielding. The number of cycles to reach the yielding transition generally increases upon reducing strain amplitude toward a critical value. As shown in Fig. 3, the maximum number of transient cycles is about 650 at the critical strain amplitude $\gamma_0 = 0.056$. The transient behavior can be rationalized as follows. When a rapidly cooled glass is initially strained up to $\gamma_{xz} = \pm\gamma_0$ in Eq. (1), the maximum stress remains relatively low and plastic deformation is homogeneously distributed within the sample. Upon further loading, the glass becomes more stable (lower potential energy at zero strain), the maximum stress increases, and the formation of a large-scale plastic event becomes more probable. We finally comment that a

better annealed $\text{Cu}_{50}\text{Zr}_{50}$ glass under cyclic loading did not yield for 700 cycles at $\gamma_0 = 0.056$, when the potential energy was $U \approx -4.951$ eV [44]. Instead, the critical strain amplitude was found to be $\gamma_0 = 0.057$ for similar loading conditions [44].

Along with the potential energy, the time dependence of shear stress, $\sigma_{xz}(t)$, was analyzed for different strain amplitudes. For each shear cycle, we computed the storage modulus, $G' = \sigma_{xz}^{max}/\gamma_0 \cos(\delta)$, where δ is the phase lag between stress and strain [51]. The variation of the storage modulus is presented in Fig. 4 for strain amplitudes below the critical value, i.e., $\gamma_0 \leq 0.055$. It can be seen that for each strain amplitude, the storage modulus increases roughly logarithmically as a function of the cycle number, which is consistent with the decay of the potential energy reported in Fig. 2. The largest increase in G' during 4000 cycles is found for the strain amplitude $\gamma_0 = 0.055$, which is just below the critical value (see Fig. 4). Similar to results for binary LJ glasses [27], the storage modulus is larger for cyclic loading at smaller strain amplitudes, where deviation from the elastic regime of deformation is reduced.

We next examine the stress-strain response of the binary glass subjected to startup continuous shear deformation with a constant strain rate of 10^{-5} ps $^{-1}$. The dependence of shear stress as a function of strain is shown in Fig. 5 after loading for 4000 cycles at the indicated strain amplitudes. For comparison, the data for the glass after rapid cooling but before cyclic deformation are also included in Fig. 5. As expected, the rapidly cooled glass under steady strain exhibits a smooth crossover to plastic flow (the violet curve in Fig. 5). By contrast, plastic flow of mechanically annealed glasses is preceded by the yielding peak, which becomes more pronounced in glasses previously loaded at larger strain amplitudes. In Fig. 6, we summarize results for the shear modulus, computed from the slope of stress-strain curves at $\gamma_{xz} \leq 0.01$, and the peak value of the stress overshoot as functions of the strain amplitude and the potential energy after 4000 cycles. It can be concluded from Fig. 6 (b) that the potential energy of the mechanically annealed glass is approximately linearly related to the magnitude of the yielding peak. On the other hand, the shear modulus remains rather insensitive to the loading amplitude, as shown Fig. 6 (c).

The storage modulus as a function of the cycle number is plotted in Fig. 7 for $\gamma_0 \geq 0.055$. Note that the data for the strain amplitude $\gamma_0 = 0.055$ are the same as in Fig. 4. It is seen in Fig. 7 that in the range $0.056 \leq \gamma_0 \leq 0.060$, cyclic loading leads to an increase in G' for a number of transient cycles, followed by the yielding transition, which is marked by an

abrupt drop in storage modulus. Interestingly, the storage modulus as a function of the cycle number at the critical strain amplitude, $\gamma_0 = 0.056$, closely follows the data for $\gamma_0 = 0.055$ during the first 600 cycles. Thus, the onset of yielding cannot be determined from the stress variation during the initial stage of deformation near the critical strain amplitude. As shown in Fig. 7, the number of transient cycles is reduced at higher strain amplitudes, $\gamma_0 > 0.056$. Overall, these results correlate well with dependence of the potential energy minima on the number of cycles reported in Fig. 3.

At the microscopic level, plastic deformation in disordered materials can be described via the so-called nonaffine displacements of atoms with respect to their neighbors [52]. In practice, the nonaffine quantity for an atom displaced from the position vector $\mathbf{r}_i(t)$ to $\mathbf{r}_i(t + \Delta t)$ during the time interval Δt is computed by minimizing the following expression:

$$D^2(t, \Delta t) = \frac{1}{N_i} \sum_{j=1}^{N_i} \left\{ \mathbf{r}_j(t + \Delta t) - \mathbf{r}_i(t + \Delta t) - \mathbf{J}_i [\mathbf{r}_j(t) - \mathbf{r}_i(t)] \right\}^2, \quad (2)$$

where \mathbf{J}_i is the transformation matrix and the sum is taken over neighboring atoms that are initially located within 4.0 \AA from $\mathbf{r}_i(t)$. It was recently shown that in glasses under periodic deformation, rearrangements of atoms become irreversible when their nonaffine displacements are greater than a cage size [20]. In addition, previous MD simulation study has indicated that the cage size is about 0.6 \AA for $\text{Cu}_{50}\text{Zr}_{50}$ metallic alloy near the glass transition temperature [53].

The dependence of the nonaffine measure as a function of the cycle number is presented in Fig. 8 for $\gamma_0 \leq 0.055$ and in Fig. 9 for $\gamma_0 \geq 0.055$. In our analysis, the nonaffine measure was computed at the beginning and end of each cycle, $\Delta t = T$ in Eq. (2), and then averaged over all atoms. For cyclic loading below the critical strain amplitude, $\gamma_0 = 0.056$, the glass evolves toward lower energy states via a sequence of plastic events, whose size is reduced at lower amplitudes, and, as a result, the average of D^2 is smaller at lower γ_0 , as shown in Fig. 8. Note that the largest fluctuations in D^2 occur at the strain amplitude $\gamma_0 = 0.055$, whereas the lower bound, $D^2 \approx 0.1 \text{ \AA}^2$, is dominated by displacements of atoms within their cages. Further, the results in the inset to Fig. 8 for the fraction of atoms with large nonaffine displacements demonstrate clearly that the number of atoms involved in plastic events decays with increasing number of cycles. By contrast, the average of D^2 increases sharply at the yielding transition for $\gamma_0 \geq 0.056$ (see Fig. 9), which is in agreement with

the critical behavior of U and G' reported in Figures 3 and 7, respectively. Moreover, after the yielding transition, plastic flow is localized within a shear band that contains a large fraction of atoms, $n_f \gtrsim 0.25$ (see Fig. 10).

The spatial organization of plastically deformed domains during the relaxation process at the strain amplitude $\gamma_0 = 0.055$ is illustrated in Fig. 11. The snapshots include configurations of atoms after n cycles at zero strain, and the colorcode denotes the magnitude of the nonaffine measure for $\Delta t = T$ in Eq. (2). Note that atoms with relatively small nonaffine displacements, $D^2[(n-1)T, T] < 0.49 \text{ \AA}^2$, were omitted for clarity, and, therefore, the void space represents elastically deformed regions. As shown in Fig. 11 (a), the transition to lower energy states initially proceeds via large irreversible displacements of atoms that form several compact clusters homogeneously distributed in the sample. Upon further loading, the total number of atoms with large nonaffine displacements is significantly reduced, see Fig. 11 (b), and eventually plastic rearrangements remain localized only in several isolated clusters, see Fig. 11 (c, d). Hence, these results demonstrate that poorly annealed glasses subjected to prolonged low-amplitude periodic deformation become more stable and reversible. On the contrary, cyclic loading at the critical strain amplitude, $\gamma_0 = 0.056$, leads to a delayed yielding transition and formation of a shear band across the whole sample, as shown in Fig. 12. A close comparison of the results for $\gamma_0 = 0.056$ in Figs. 10 and 12 reveals details of the yielding transition; namely, shear band initiation [$n_f = 0.07$ in Fig. 12 (b)], propagation of plastic regions along the yz plane [$n_f = 0.20$ in Fig. 12 (c)], and formation of a fully developed shear band [$n_f = 0.28$ in Fig. 12 (d)]. Together, these findings emphasize the role of plastic rearrangements in structural relaxation and yielding of metallic glasses under cyclic loading.

IV. CONCLUSIONS

In summary, we investigated the critical behavior and mechanical annealing of a Cu-Zr metallic glass subjected to periodic shear deformation by means of molecular dynamics simulations. The glass was prepared via rapid cooling from the liquid state to room temperature and then subjected to oscillatory shear at strain amplitudes ranged from slightly above to well below a critical value. It was found that low-amplitude cyclic loading gradually relocates the glass to lower energy states, and the storage modulus approximately follows a

logarithmic dependence on the number of shear cycles. In addition, we showed that the potential energy after four thousand shear cycles depends linearly on the yielding stress of the annealed glass under monotonic shear deformation. The structural relaxation proceeds via a sequence of plastic rearrangements of clusters of atoms whose typical size is larger at higher strain amplitudes. By contrast, when the strain amplitude is greater than a critical value, the glass is mechanically annealed for a number of cycles followed by an abrupt increase in the potential energy due to flow localization within a shear band. The formation of the shear band is accompanied with the increase of the fraction of atoms with large nonaffine displacements and a drop in storage modulus.

Acknowledgments

The financial support from the National Science Foundation (CNS-1531923) is gratefully acknowledged. MD simulations were carried out at the Wright State University's Computing Facility and the Ohio Supercomputer Center using the LAMMPS code [50].

-
- [1] K. Gao, X. G. Zhu, L. Chen, W. H. Li, X. Xu, B. T. Pan, W. R. Li, W. H. Zhou, L. Li, W. Huang, and Y. Li, Recent development in the application of bulk metallic glasses, *J. Mater. Sci. Technol.* **131**, 115 (2022).
 - [2] H. Jiang, T. Shang, H. Xian, B. Sun, Q. Zhang, Q. Yu, H. Bai, L. Gu, and W. Wang, Functional properties of amorphous alloys, *Small Struct.* **2**, 2000057 (2021).
 - [3] T. Egami, T. Iwashita, and W. Dmowski, Mechanical properties of metallic glasses, *Metals* **3**, 77 (2013).
 - [4] J. C. Qiao, Q. Wang, J. M. Pelletier, H. Kato, R. Casalini, D. Crespo, E. Pineda, Y. Yao, Y. Yang, Structural heterogeneities and mechanical behavior of amorphous alloys, *Prog. Mater. Sci.* **104**, 250 (2019).
 - [5] T. C. Hufnagel, C. A. Schuh, and M. L. Falk, Deformation of metallic glasses: Recent developments in theory, simulations, and experiments, *Acta Materialia* **109**, 375 (2016).
 - [6] H. Jia, G. Wang, S. Chen, Y. Gao, W. Li, and P. K. Liaw, Fatigue and fracture behavior of bulk metallic glasses and their composites, *Prog. Mater. Sci.* **98**, 168 (2018).

- [7] B. C. Menzel and R. H. Dauskardt, Stress-life fatigue behavior of a Zr-based bulk metallic glass, *Acta Mater.* **54**, 935 (2006).
- [8] Z. Sha, W. Lin, L. H. Poh, G. Xing, Z. Liu, T. Wang, and H. Gao, Fatigue of metallic glasses, *Appl. Mech. Rev.* **72**, 050801 (2020).
- [9] Y. Sun, A. Concustell, and A. L. Greer, Thermomechanical processing of metallic glasses: Extending the range of the glassy state, *Nat. Rev. Mater.* **1**, 16039 (2016).
- [10] S. V. Ketov, Y. H. Sun, S. Nachum, Z. Lu, A. Checchi, A. R. Beraldin, H. Y. Bai, W. H. Wang, D. V. Louzguine-Luzgin, M. A. Carpenter, and A. L. Greer, Rejuvenation of metallic glasses by non-affine thermal strain, *Nature* **524**, 200 (2015).
- [11] R. M. O. Mota, E. T. Lund, S. Sohn, D. J. Browne, D. C. Hofmann, S. Curtarolo, A. van de Walle, and J. Schroers, Enhancing ductility in bulk metallic glasses by straining during cooling, *Commun. Mater.* **2**, 23 (2021).
- [12] N. V. Priezjev, Cooling under applied stress rejuvenates amorphous alloys and enhances their ductility, *Metals* **11**, 67 (2021).
- [13] A. A. Abdu Aliyu, C. Panwisawas, J. Shinjo, C. Puncreobutr, R. C. Reed, K. Pongsiri, and B. Lohwongwatana, Laser-based additive manufacturing of bulk metallic glasses: recent advances and future perspectives for biomedical applications, *J. Mater. Res. Technol.* **23**, 2956 (2023).
- [14] N. V. Priezjev, Heterogeneous relaxation dynamics in amorphous materials under cyclic loading, *Phys. Rev. E* **87**, 052302 (2013).
- [15] I. Regev, T. Lookman, and C. Reichhardt, Onset of irreversibility and chaos in amorphous solids under periodic shear, *Phys. Rev. E* **88**, 062401 (2013).
- [16] D. Fiocco, G. Foffi, and S. Sastry, Oscillatory athermal quasistatic deformation of a model glass, *Phys. Rev. E* **88**, 020301(R) (2013).
- [17] I. Regev, J. Weber, C. Reichhardt, K. A. Dahmen, and T. Lookman, Reversibility and criticality in amorphous solids, *Nat. Commun.* **6**, 8805 (2015).
- [18] J. Luo, K. Dahmen, P. K. Liaw, and Y. Shi, Low-cycle fatigue of metallic glass nanowires, *Acta Mater.* **87**, 225 (2015).
- [19] Z. D. Sha, S. X. Qu, Z. S. Liu, T. J. Wang, and H. Gao, Cyclic deformation in metallic glasses, *Nano Lett.* **15**, 7010 (2015).
- [20] N. V. Priezjev, Reversible plastic events during oscillatory deformation of amorphous solids,

- Phys. Rev. E **93**, 013001 (2016).
- [21] T. Kawasaki and L. Berthier, Macroscopic yielding in jammed solids is accompanied by a non-equilibrium first-order transition in particle trajectories, Phys. Rev. E **94**, 022615 (2016).
- [22] N. V. Priezjev, Nonaffine rearrangements of atoms in deformed and quiescent binary glasses, Phys. Rev. E **94**, 023004 (2016).
- [23] P. Leishangthem, A. D. S. Parmar, and S. Sastry, The yielding transition in amorphous solids under oscillatory shear deformation, Nat. Commun. **8**, 14653 (2017).
- [24] N. V. Priezjev, Collective nonaffine displacements in amorphous materials during large-amplitude oscillatory shear, Phys. Rev. E **95**, 023002 (2017).
- [25] S. Dagois-Bohy, E. Somfai, B. P. Tighe, and M. van Hecke, Softening and yielding of soft glassy materials, Soft Matter **13**, 9036 (2017).
- [26] N. V. Priezjev, Molecular dynamics simulations of the mechanical annealing process in metallic glasses: Effects of strain amplitude and temperature, J. Non-Cryst. Solids **479**, 42 (2018).
- [27] N. V. Priezjev, The yielding transition in periodically sheared binary glasses at finite temperature, Comput. Mater. Sci. **150**, 162 (2018).
- [28] A. D. S. Parmar, S. Kumar, and S. Sastry, Strain localization above the yielding point in cyclically deformed glasses, Phys. Rev. X **9**, 021018 (2019).
- [29] N. V. Priezjev, Slow relaxation dynamics in binary glasses during stress-controlled, tension-compression cyclic loading, Comput. Mater. Sci. **153**, 235 (2018).
- [30] N. V. Priezjev, Accelerated relaxation in disordered solids under cyclic loading with alternating shear orientation, J. Non-Cryst. Solids **525**, 119683 (2019).
- [31] N. V. Priezjev, Shear band formation in amorphous materials under oscillatory shear deformation, Metals **10**, 300 (2020).
- [32] W. T. Yeh, M. Ozawa, K. Miyazaki, T. Kawasaki, and L. Berthier, Glass stability changes the nature of yielding under oscillatory shear, Phys. Rev. Lett. **124**, 225502 (2020).
- [33] N. V. Priezjev, Alternating shear orientation during cyclic loading facilitates yielding in amorphous materials, J. Mater. Eng. Perform. **29**, 7328 (2020).
- [34] N. V. Priezjev, A delayed yielding transition in mechanically annealed binary glasses at finite temperature, J. Non-Cryst. Solids **548**, 120324 (2020).
- [35] H. Bhaumik, G. Foffi, and S. Sastry, The role of annealing in determining the yielding behavior of glasses under cyclic shear deformation, PNAS **118**, 2100227118 (2021).

- [36] N. V. Priezjev, Accessing a broader range of energy states in metallic glasses by variable-amplitude oscillatory shear, *J. Non-Cryst. Solids* **560**, 120746 (2021).
- [37] N. V. Priezjev, Yielding transition in stable glasses periodically deformed at finite temperature, *Comput. Mater. Sci.* **200**, 110831 (2021).
- [38] S. Cui, H. Liu, and H. Peng, Anisotropic correlations of plasticity on the yielding of metallic glasses, *Phys. Rev. E* **106**, 014607 (2022).
- [39] P. Das, A. D. S. Parmar, and S. Sastry, Annealing glasses by cyclic shear deformation, *J. Chem. Phys.* **157**, 044501 (2022).
- [40] N. V. Priezjev, Mechanical annealing and yielding transition in cyclically sheared binary glasses, *J. Non-Cryst. Solids* **590**, 121697 (2022).
- [41] B. Shang, N. Jakse, P. Guan, W. Wang, and J.-L. Barrat, Influence of oscillatory shear on nucleation in metallic glasses: A molecular dynamics study, *Acta Mater.* **246**, 118668 (2023).
- [42] N. V. Priezjev, Fatigue failure of amorphous alloys under cyclic shear deformation, *Comput. Mater. Sci.* **226**, 112230 (2023).
- [43] V. V. Krishnan, K. Ramola, and S. Karmakar, Annealing effects of multidirectional oscillatory shear in model glass formers, *Phys. Rev. Applied* **19**, 024004 (2023).
- [44] N. V. Priezjev, Fatigue behavior of Cu-Zr metallic glasses under cyclic loading, *Metals* **13**, 1606 (2023).
- [45] L. Zella, J. Moon, and T. Egami, Ripples in the bottom of the potential energy landscape of metallic glass, *Nat. Commun.* **15**, 1358 (2024).
- [46] X. C. Tang and X. H. Yao, The effect of forced vibration coupling on amorphous alloy superplasticity, *J. Non-Cryst. Solids* **630**, 122905 (2024).
- [47] Y. Q. Cheng, E. Ma, and H. W. Sheng, Atomic level structure in multicomponent bulk metallic glass, *Phys. Rev. Lett.* **102**, 245501 (2009).
- [48] Y. Q. Cheng and E. Ma, Atomic-level structure and structure-property relationship in metallic glasses, *Prog. Mater. Sci.* **56**, 379 (2011).
- [49] Z. Fan and E. Ma, Predicting orientation-dependent plastic susceptibility from static structure in amorphous solids via deep learning, *Nat. Commun.* **12**, 1506 (2021).
- [50] S. J. Plimpton, Fast parallel algorithms for short-range molecular dynamics, *J. Comp. Phys.* **117**, 1 (1995).
- [51] K. Hyun, M. Wilhelm, C. O. Klein, K. S. Cho, J. G. Nam, K. H. Ahn, S. J. Lee, R. H. Ewoldt,

- and G. H. McKinley, A review of nonlinear oscillatory shear tests: Analysis and application of large amplitude oscillatory shear (LAOS), *Prog. Polym. Sci.* **36**, 1697 (2011).
- [52] M. L. Falk and J. S. Langer, Dynamics of viscoplastic deformation in amorphous solids, *Phys. Rev. E* **57**, 7192 (1998).
- [53] X. Wang, W.-S. Xu, H. Zhang, and J. F. Douglas, Universal nature of dynamic heterogeneity in glass-forming liquids: A comparative study of metallic and polymeric glass-forming liquids, *J. Chem. Phys.* **151**, 184503 (2019).

Figures

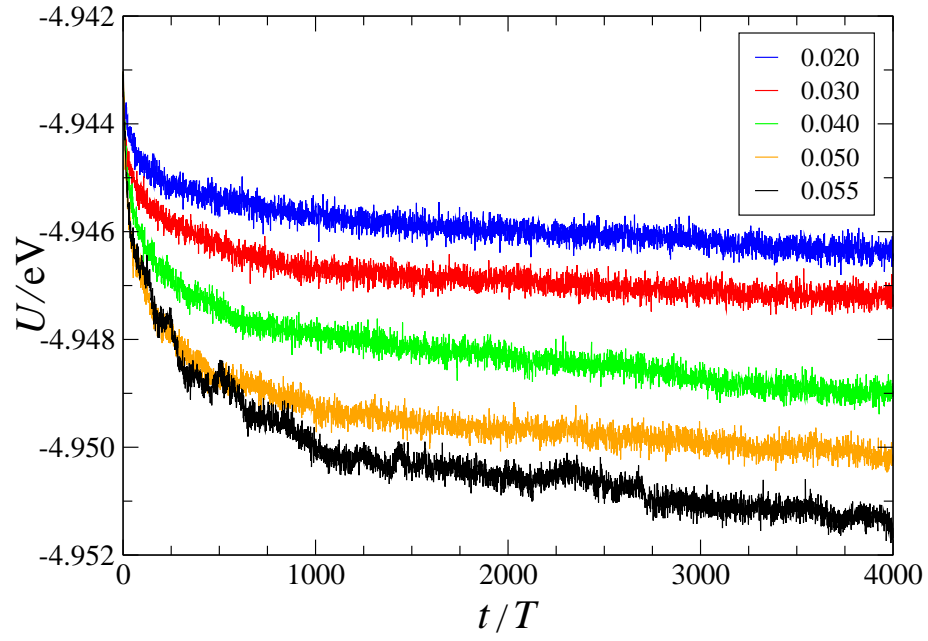


FIG. 1: The potential energy at the end of each cycle versus cycle number for the indicated strain amplitudes γ_0 . The period of oscillation is $T = 1.0$ ns.

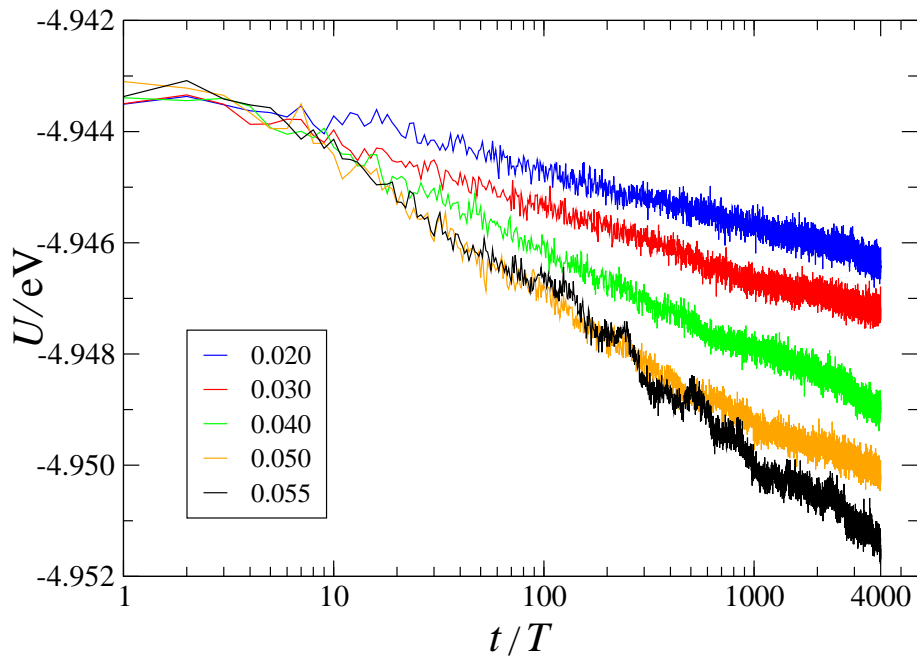


FIG. 2: A linear-log plot of the same data as in Fig. 1.

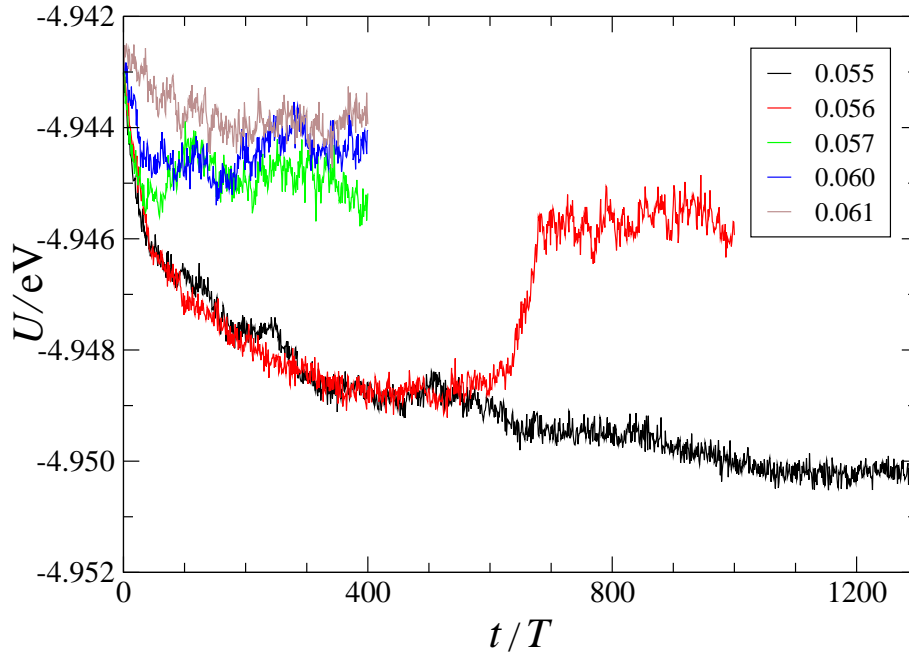


FIG. 3: The variation of potential energy when strain is zero as a function of the number of cycles for strain amplitudes $\gamma_0 = 0.055, 0.056, 0.057, 0.060$ and 0.061 . The data for $\gamma_0 = 0.055$ are the same as in Fig. 1.

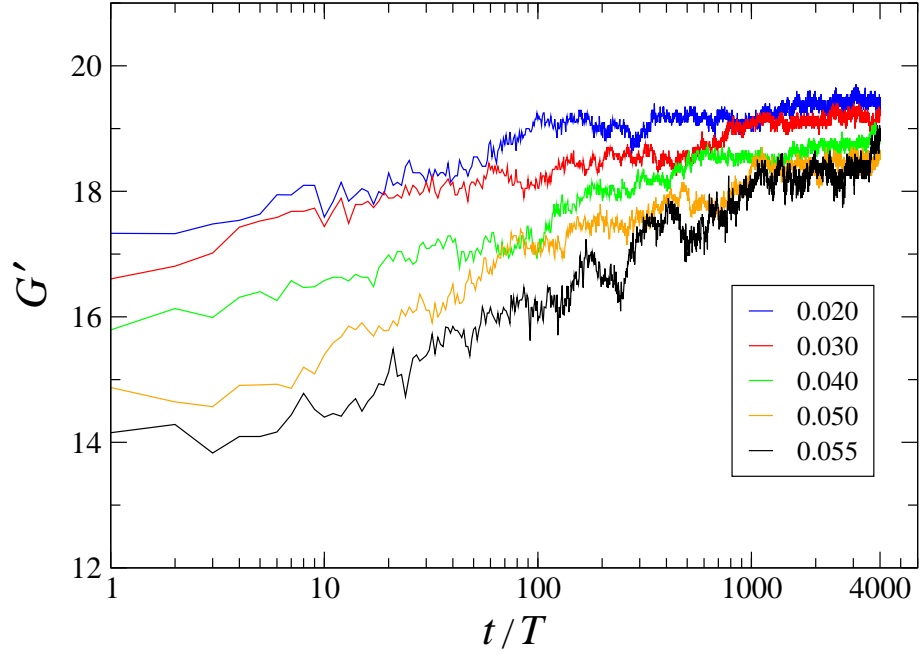


FIG. 4: The storage modulus G' (in units of GPa) as a function of the cycle number for the indicated values of the strain amplitude γ_0 . The period of oscillation is $T = 1.0$ ns.

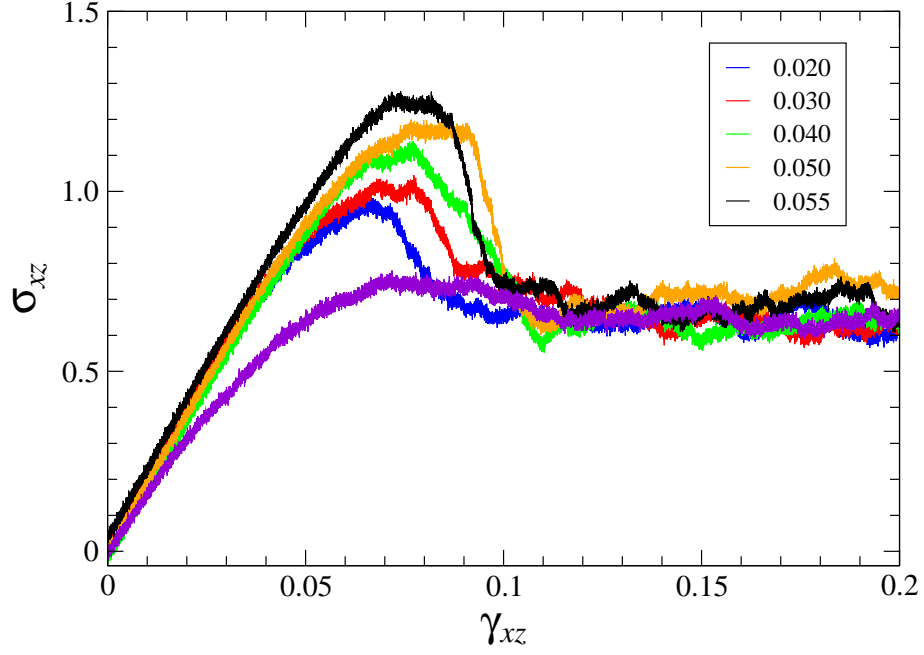


FIG. 5: Shear stress, σ_{xz} (in units of GPa), versus strain for glasses deformed at a constant strain rate of 10^{-5} ps^{-1} after 4000 cycles at indicated γ_0 . The lower violet curve is the data before cyclic loading.

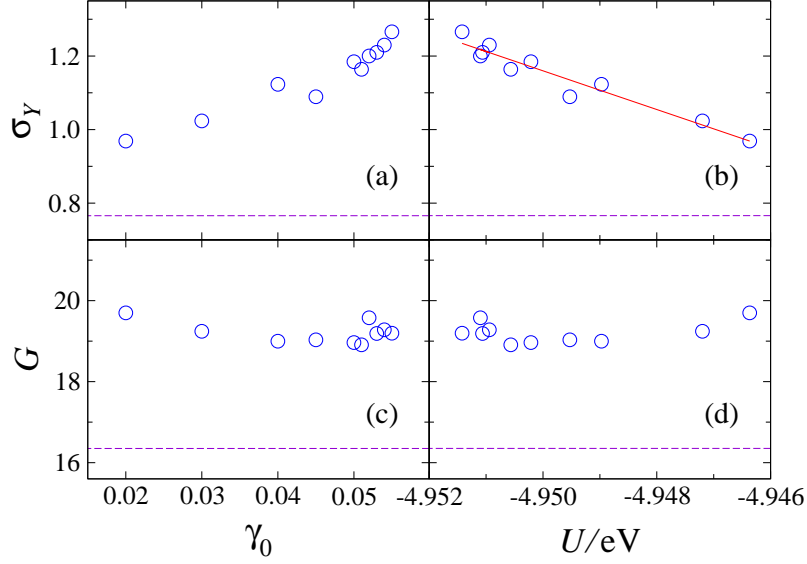


FIG. 6: The shear modulus, G (in GPa), and the peak value of the stress overshoot, σ_Y (in GPa), as functions of the strain amplitude, γ_0 , and the potential energy after 4000 loading cycles, U . The horizontal dashed lines indicate G and σ_Y for the steadily sheared glass before cyclic loading was applied. The straight red line in the panel (b) is the best fit to the data.

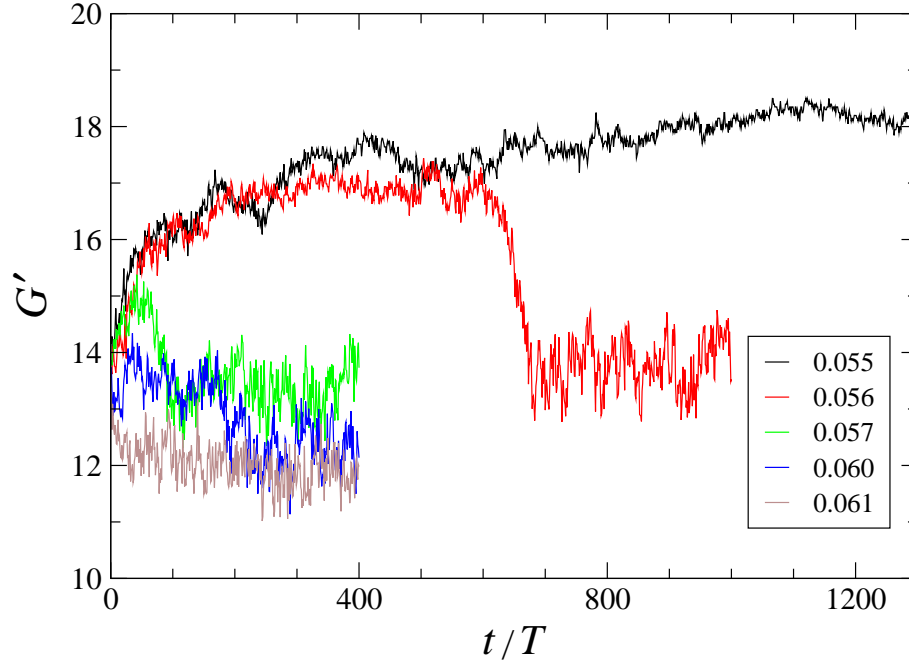


FIG. 7: The storage modulus G' (in units of GPa) versus cycle number for strain amplitudes $\gamma_0 \geq 0.055$. The data for G' at $\gamma_0 = 0.055$ are the same as in Fig. 4. The oscillation period is $T = 1.0$ ns.

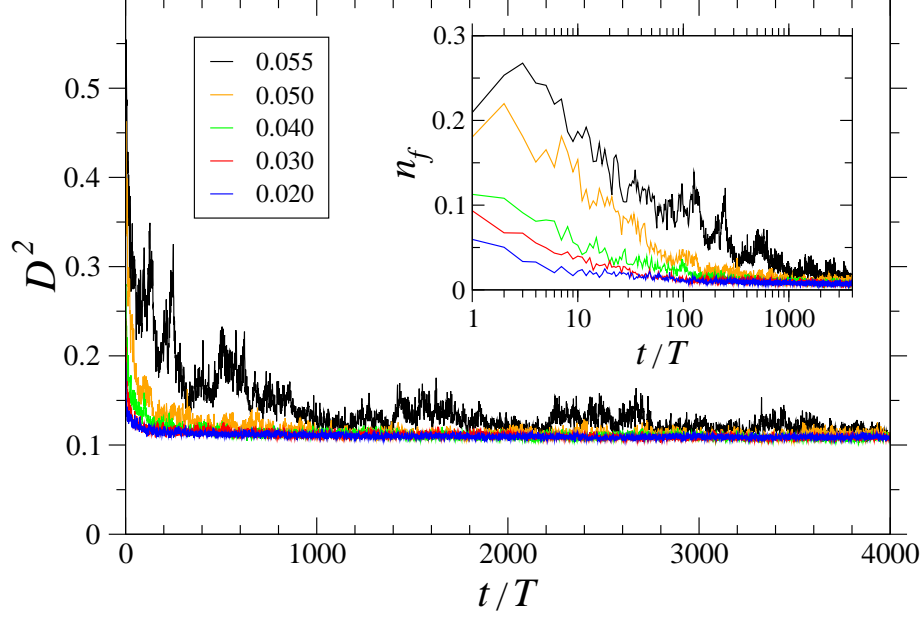


FIG. 8: The average of the nonaffine quantity, $D^2[(n-1)T, T]$ (in units of \AA^2), as a function of the number of cycles for the indicated strain amplitudes. The oscillation period is $T = 1.0$ ns. The inset shows the fraction of atoms with $D^2[(n-1)T, T] > 0.49 \text{\AA}^2$ versus cycle number for the same strain amplitudes.

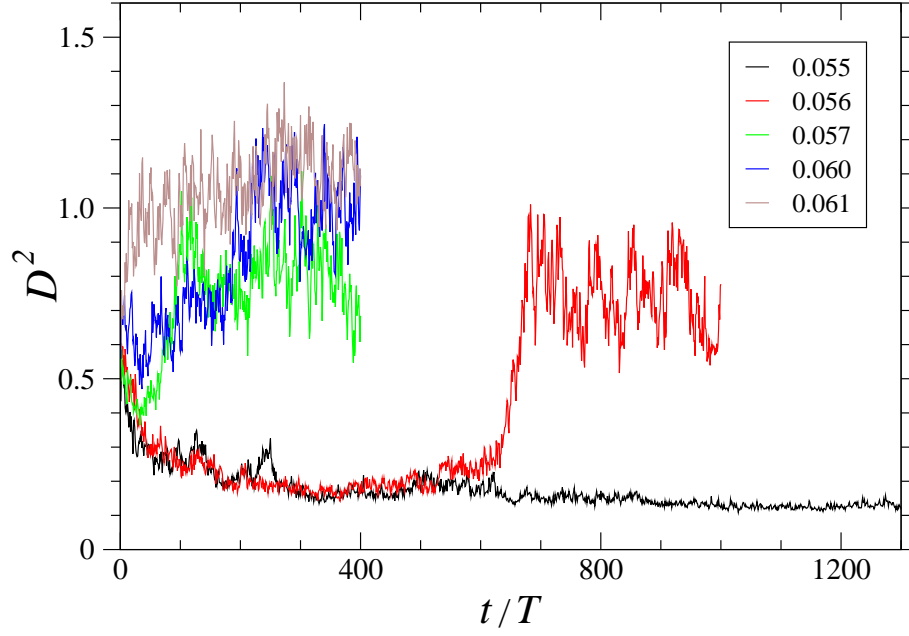


FIG. 9: The average of $D^2[(n-1)T, T]$ (in units of \AA^2) versus number of cycles for strain amplitudes $\gamma_0 \geq 0.055$. The data for the strain amplitude $\gamma_0 = 0.055$ (the black curve) are the same as in Fig. 8.

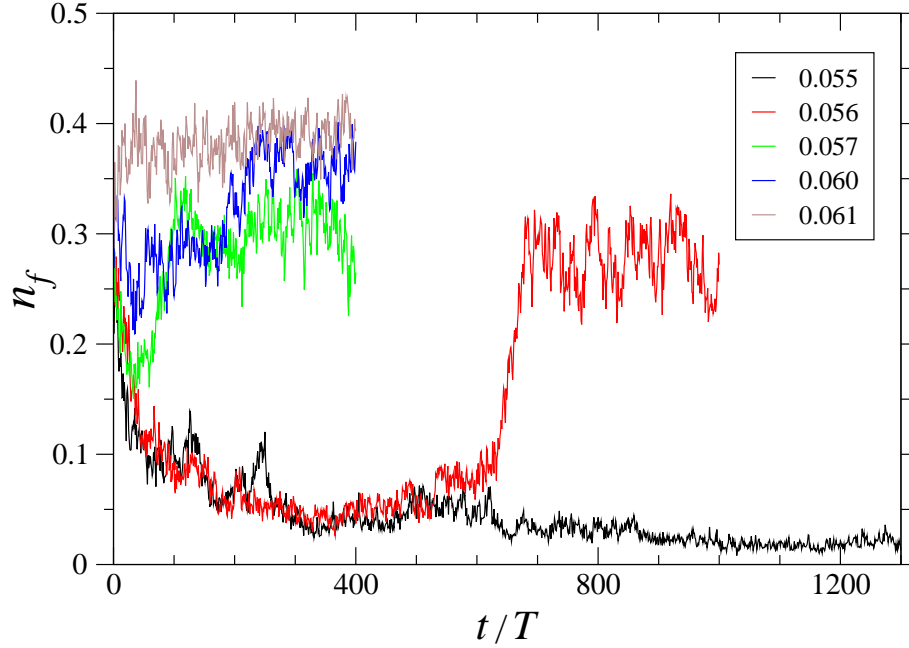


FIG. 10: The fraction of atoms with large nonaffine displacements, $D^2[(n-1)T, T] > 0.49 \text{ \AA}^2$, as a function of the number of cycles for the tabulated strain amplitudes. The oscillation period is $T = 1.0 \text{ ns}$.

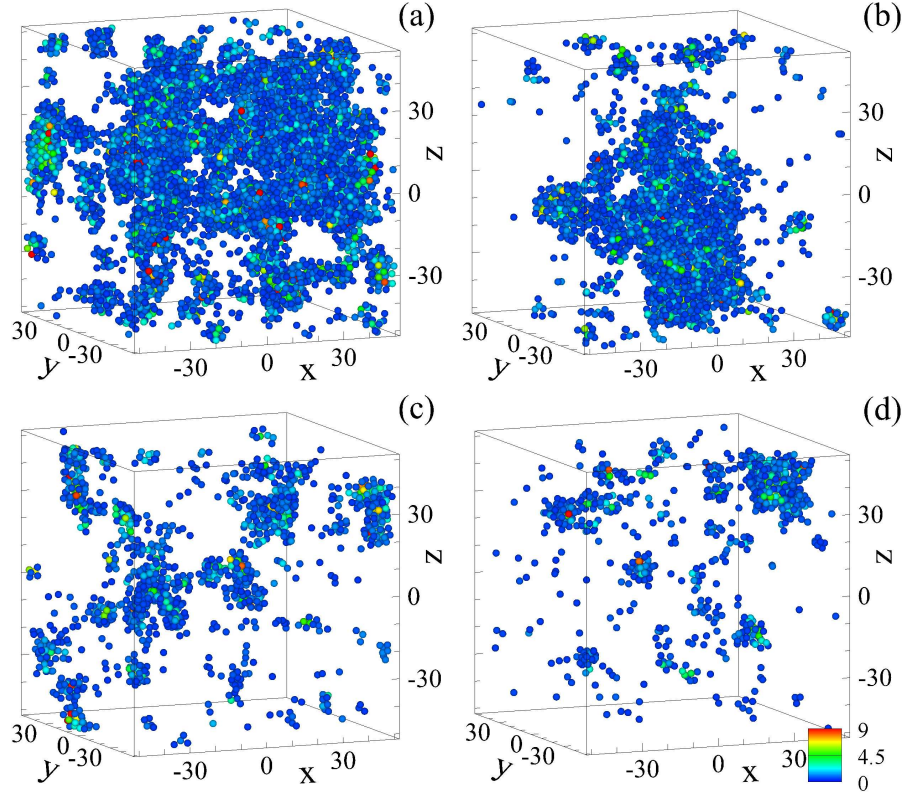


FIG. 11: Selected configurations of atoms in the $\text{Cu}_{50}\text{Zr}_{50}$ glass loaded at the strain amplitude $\gamma_0 = 0.055$. The nonaffine quantity is (a) $D^2(50T, T) > 0.49 \text{ \AA}^2$, (b) $D^2(500T, T) > 0.49 \text{ \AA}^2$, (c) $D^2(1000T, T) > 0.49 \text{ \AA}^2$, and (d) $D^2(3000T, T) > 0.49 \text{ \AA}^2$. Cu and Zr atoms are not drawn to scale. The legend in the panel (d) indicates the magnitude of the nonaffine quantity.

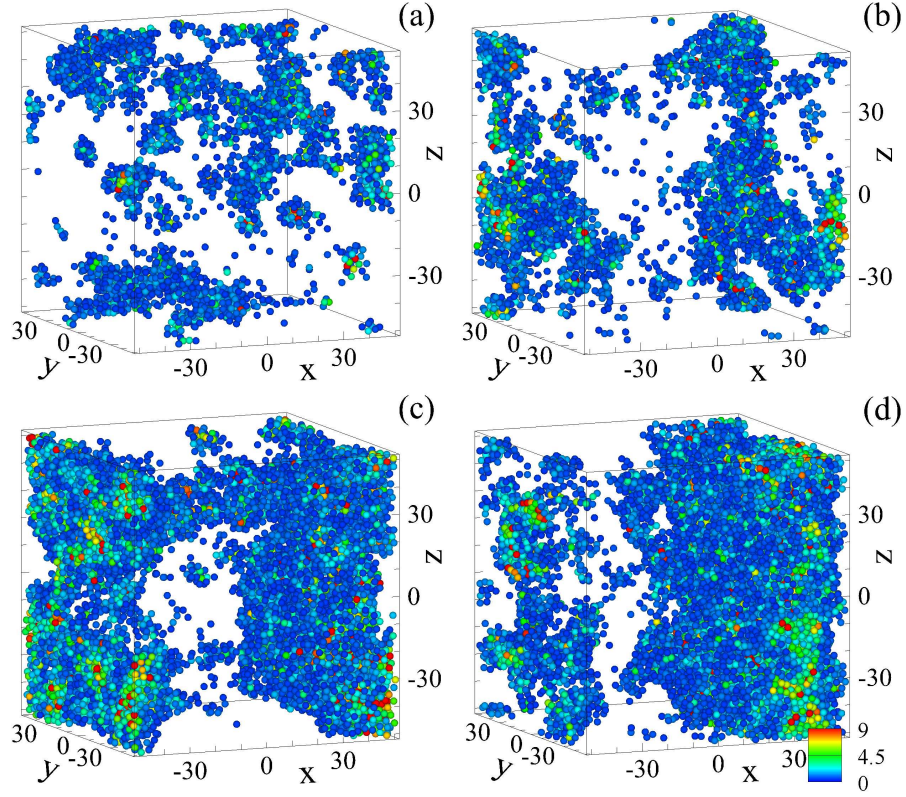


FIG. 12: Snapshots of atomic configurations of the binary glass periodically deformed at the critical strain amplitude $\gamma_0 = 0.056$. The nonaffine measure is (a) $D^2(300T, T) > 0.49 \text{ \AA}^2$, (b) $D^2(600T, T) > 0.49 \text{ \AA}^2$, (c) $D^2(660T, T) > 0.49 \text{ \AA}^2$, and (d) $D^2(800T, T) > 0.49 \text{ \AA}^2$. Atoms are not depicted to scale. The colorcode is the same as in Fig. 11.